Journal of Nuclear Medicine, published on May 24, 2018 as doi:10.2967/jnumed.116.185967

The Immuno-Imaging Toolbox

Aaron T. Mayer[1], and Sanjiv S. Gambhir[1,2]

[1]Department of Bioengineering, Stanford University, Stanford, California

[2]Department of Radiology, Department of Materials Science & Engineering, Molecular Imaging Program at Stanford, Canary Center at Stanford for Cancer Early Detection, Stanford University, Stanford, California

Corresponding author: Sanjiv Sam Gambhir, MD, PhD; Chair, Department of Radiology, Director, Molecular Imaging Program at Stanford (MIPS); Director, Cancer Center at Stanford for Early Cancer Detection, Professor, Department of Radiology, The James H Clark Center, 318 Campus Drive, East Wing 1st Floor, Stanford, CA 94305; Email: sgambhir@stanford.edu

Noteworthy

- The immuno-imaging toolbox is rapidly expanding and providing novel insights into the immune system and immune responses to therapy.
- Tables 1 and 2 provide a comprehensive overview of the current state-of-art immuno-imaging toolbox.
- Clinical roles for the immuno-imaging toolbox include guiding rationale drug development, informing optimal treatment strategies, improving patient stratification/ trial design, providing early clinical response predictions and monitoring therapeutic outcomes for better patient management.

Abstract. The Immuno-Imaging Toolbox

The recent clinical success of cancer immunotherapy has renewed interest in the development of tools to image the immune system. In general, immunotherapies attempt to enable the body's own immune cells to seek out and destroy malignant disease. Molecular imaging of the cells and molecules which regulate immunity could provide unique insight into the mechanisms of action, *and failure*, of immunotherapies. In this review, we will collectively refer to the tools applied towards imaging the immune system as the immuno-imaging toolbox. The immuno-imaging toolbox is comprised of imaging hardware, software, and biological wetware which together enable dynamic and non-invasive visualization of immune response. Other recent reviews have focused on specific portions of the immuno-imaging toolbox, including advances in imaging hardware (*1*) and certain classes of imaging probes (*2*,*3*). Here we will attempt to provide a comprehensive overview of the current state-of-the-art immuno-imaging toolbox with a focus on imaging strategies and their applications towards immunotherapy.

Part I. Immuno-Imaging Strategies

The immuno-imaging toolbox has rapidly expanded over the last decade due to a shift in focus from imaging cancer and specific diseases to a patient's underlying immune state. This paradigm shift has been driven in part by the failure of conventional imaging methods to accurately monitor and predict response to clinical immunotherapies. Since the success of immunotherapy is dependent upon the generation of a robust immune response, immuno-imaging tools are of high interest. Tables 1 & 2 attempt to summarize the current status of the immuno-imaging toolbox by providing a comprehensive list of agents which have

been utilized to image the immune system (Tables 1 and 2). The tables divide the immuno-imaging toolbox into two strategic classes: 1) probes targeted for endogenous immune cell biomarkers, and 2) immune cell labeling (direct and indirect approaches). Here we discuss the implementation of each strategy towards imaging immune cells and molecules (Fig. 1).

I.1 Probes targeted for endogenous immune cell biomarkers.

These approaches seek to develop molecular imaging agents that bind to, or are selectively taken up by, endogenous immune molecules or immune cells respectively. There are a wide variety of immune targets to choose from, many of which have been categorized by immunologists as cluster of differentiation (CD) markers. The expression of CD markers is spatially and temporally heterogeneous and together these markers define an immune cells phenotype. CD markers can be used to identify anything from general immune cell classes (e.g. $CD3^+$ T cells), to specific cell subsets (e.g. $CD3^+CD4^+FoxP3^+$ regulatory T cells), and immune cell states (e.g. $CD3^+CD4^+CD25^+CD279^{hi}FOXP3^+$ activated regulatory T cells). In addition to these CD markers, certain metabolic pathways are also selectively upregulated in immune cells. For example, both deoxyguanosine kinase and deoxycytidine kinase, implicated in nucleoside salvage pathways, have been identified as being highly upregulated in activated, as compared to resting T cells. The identification and selection of immune biomarkers is an active and important area of research. Due to the natural presence of these immune markers, probes targeted for endogenous immune cell biomarkers provide a relatively straightforward immuno-imaging approach.

Endogenous biomarker targeting probes can be built from antibodies and other natural protein scaffolds, as well as developed de novo from chemical or protein engineering techniques. Large libraries of potential binders are often generated and screened against an immune target of interest. Due to the challenges of developing small molecule chemical libraries, biologics (antibodies or their derivatives) have become a favorite option for imaging the immune system. Often, antibodies already under development for immunotherapeutic applications can quickly be modified for imaging via conjugation to a contrast agent or radionuclide. Another benefit of antibodies as imaging agents is their naturally high specificity and binding affinity towards their cognate antigen. Drawbacks to antibody imaging include their large size (~150kDa) leading to slow clearance from non-target tissues and relatively poor penetration into target tissues. When

imaging with antibodies, a clinician must often wait several days before the background signal from unbound probe has cleared from various tissues and the circulation. To overcome these challenges, alternative biologic scaffolds are being developed and optimized for improved pharmacokinetics. Engineered antibody fragments such as minibodies, diabodies, and scFv fragments (*4*), and antibodies from other species such as camelid and shark, are all actively being explored (*5*). Endogenous ligands can be affinity matured and modified to be used as probes (*6*), and aptamers, adnectins, and cystine knots add to a growing list of scaffolds which are being developed and applied towards immuno-imaging. With all of these potential scaffolds to choose from, one must weigh the trade-offs between specificity, sensitivity and clearance. Mounting empirical data from preclinical studies as well as mathematical models (*7*) should help identify the ideal scaffold choices for immuno-imaging applications in the clinic.

I.2 Immune cell labeling strategies

Direct labeling of immune cells ex vivo that have been first isolated from a patient is another commonly utilized immuno-imaging technique. In this method, immune cells are incubated ex vivo with an imaging agent before being adoptively transferred back into the patient. The immune cells can then be tracked longitudinally by imaging over time. A wide range of immune cells have been monitored in this manner including T cells, B cells, natural killer cells, dendritic cells, macrophage, monocytes, and hematopoietic stem cells. While this strategy enables simple and specific labeling of almost any chosen immune cell of interest, it has several drawbacks. Many contrast agents used in this manner have a direct impact on cell function. For example, both Indium Oxine and Feuromoxytol used for tracking cells via PET or MRI respectively, are known to cause cell cytotoxicity at too high of concentrations. Furthermore, once successfully labeled, there is a loss in sensitivity over time due to efflux or dilution of the probe during cell division. In clinical practice, this phenomenon limits the amount of time cells can be monitored from hours to weeks following adoptive transfer. Finally, once the cells have been transferred back into the patient, it is impossible to tell whether the immune cells are viable (a dead cell will still lead to signal with this technique), further confounding the interpretation of response. None the less, direct labeling is an important imaging technique which has provided valuable insights into immune cell reconstitution and cell homing to sites of disease or damage.

Indirect labeling approaches overcome many of the challenges associated with direct labeling. This labeling strategy involves either viral transduction or transfection of a reporter gene into an immune cell of interest. A reporter gene can be anything from a luciferase (e.g., the enzyme used by fireflies which enables their characteristic bioluminescent glow), to viral genes which code for enzymes not commonly found in the human body. A successful example has been herpes simplex virus type 1 thymidine kinase, which can subsequently be visualized using a reporter probe which is trapped by only cells expressing that reporter gene. Furthermore, reporter genes can be put downstream of promoters which "turn-on" the expression of the gene only if an immune cell is activated. In this way, reporter gene strategies can reveal immune cell location(s), viability, and activation state. Reporter genes have been developed for use with multiple imaging modalities including MRI, PET, and optical imaging (*8*). While indirect labeling techniques can theoretically be performed in vivo, challenges with specificity and concerns regarding viral gene editing in humans has limited their primary application to ex vivo immune cell manipulation. As with direct labeling techniques, it is critical to assess that the introduction of the reporter gene is not affecting the viability or function of the immune cell itself. Other issues with using viruses or transfection techniques including challenges with stable expression and gene transcription "leakiness", as well as the need to remove cells from a patient have partially limited the applications of this technique thus far. That said, as the safety and efficacy of certain viruses improves, we may see more widespread clinical adoption of this imaging technique due to the ability to image immune cells for their entire lifespan.

Part II. Immuno-Imaging Applications Towards Immunotherapy

The immuno-imaging strategies discussed above are rapidly being deployed in an attempt to predict and monitor response to immunotherapy. In this section we will review several classes of immunotherapy (Fig. 2) and provide examples of how immuno-imaging is already being applied to better understand and characterize immune response (Fig. 3).

II.1 Immune checkpoint blockade.

Immune checkpoint blockade (ICB) has emerged as a promising immunotherapeutic treatment strategy for a number of malignancies. Under normal physiologic conditions, so called immune checkpoints help prevent the immune system from erroneously attacking healthy tissues. Unfortunately,

cancers have evolved to upregulate immune checkpoint molecules to evade immune detection and destruction. By blocking these immunosuppressive signaling pathways with therapeutic drugs, ICB strategies enable the formation of an optimal therapeutic anti-tumor immune responses. ICB has led to unprecedented clinical success in patients with late stage melanoma, non-small cell lung cancer, and bladder cancer. Numerous clinical trials are under way and the Federal Drug Administration (FDA) has already approved drugs targeting the immune checkpoint molecules cytotoxic T-lymphocyte antigen-4 (CTLA-4), programmed death-1 (PD-1), and programmed death-ligand-1 (PD-L1) (*9*). Despite the success of immune checkpoint blockade, only a subset of patients respond.

A number of tools are being developed in hopes of predicting which patients are most likely to respond to ICB therapy. Probes targeted for endogenous immune cell biomarkers are particularly well suited towards measuring the dynamic and heterogenous expression of immune checkpoint molecules. Numerous imaging agents have been developed and applied in an attempt to non-invasively interrogate PD-1, PD-L1 and CTLA-4 expression. For example, Heskamp et. al. demonstrate the successful development of a monoclonal antibody labeled with Indium-111 for SPECT/CT imaging of human PD-L1 expression in mice (*10*). Their mouse images showed heterogenous uptake which correlated well with PD-L1 expression in multiple types of human tumor xenografts. They concluded that the technique may enable better patient selection for PD-1 and PD-L1 targeted therapy in the future. In addition to measuring the expression of immune checkpoint molecules, the presence of immune cells before and/or after ICB therapy may correlate with therapeutic response. Rashidian et. al. show that 89Zr-labeled PEGylated single-domain antibody fragments (VHHs) specific for CD8 enable ImmunoPET tracking of cytotoxic T cells (*11*). While the absolute number of intra-tumoral CD8 T cells measured by PET imaging did not correlate well with therapeutic response to CTLA-4 checkpoint blockade, the distribution of T cells in the tumor did. Homogenous uptake patterns, indicative of good T cell penetration and tumor coverage, stratified responders from non-responders in this study. It is likely that both immune checkpoint expression and immune cell intratumoral distribution will provide valuable insights into clinical patient responses to ICB therapy.

II.2 Chimeric antigen receptor T cells.

Chimeric antigen receptor T cells (CAR-T) represent a personalized therapeutic approach in which T cells are removed from a patient and genetically engineered to express a chimeric antigen receptor, before being introduced back into the patient. Chimeric antigen receptors have been designed to bind a variety of tumor associated antigens. Newer generations of CAR-Ts have coupled these extracellular binding domains to intracellular costimulatory moieties, improving therapeutic potency and efficacy. Thus far, CAR-T cell strategies have seen the greatest success in treating hematologic malignancies while they have struggled to find efficacy in solid tumors. In addition, CAR-T therapies often present with severe side effects including cytokine release syndrome, neurologic toxic effects, and in some cases, even death (*12*). “On-target, off-tumor” toxicity is another common concern. For example, CAR-Ts targeting CD19 will not only eradicate malignant CD19+ B cells but also normal CD19+ B cells leading to B cell aplasia. Despite durable remissions in certain patients, approximately half will exhibit relapse. The reasons for variations in patient response are not well understood at this point in time, though they are likely linked to CAR-T durability, antigen loss, and on-target off-tumor effects.

Reporter gene imaging strategies lend themselves readily to CAR-T therapy, as the cells already need to be removed from the patient and genetically engineered. KV Keu et. al. recently demonstrated reporter gene imaging of CAR-T cells in glioblastoma patients (*13*,*14*). In this study, cytotoxic T cells bearing the chimeric antigen reception interleukin-13 zetakine for IL-13Rα^{+} tumor targeting were engineered to also express HSV1-tk as a dual-purpose suicide and imaging reporter gene. ^{18}F-FHBG PET imaging was subsequently utilized to longitudinally monitor CAR-T trafficking, survival and proliferation in multiple patients with recurrent high-grade gliomas. While this study faced many challenges including strict FDA regulations limiting the number of scans and access to patients, it provides a proof of principle that reporter gene imaging may one day be able to link CTL trafficking and viability to tumor response and patient survival, guiding both the development and application of CAR therapy for the treatment of solid tumors.

II.3 Dendritic cell vaccines.

Dendritic cell (DC) vaccines comprise a special class of immunotherapy in which professional antigen presenting cells, known as DCs, are loaded ex vivo with an antigen/s and then adoptively

transferred back to the patient. When successful, the antigen loaded DCs lead to the generation of an adaptive immune response against the target antigen of interest. In order for these therapies to be effective though, the dendritic cells must migrate through the lymphatic system to lymph nodes where they can present the antigen and activate effector immune cells. Successful homing to secondary lymphoid organs represents an intermediate endpoint which could be used to improve or predict the success of dendritic cell vaccine strategies.

Direct cell labeling and imaging is well suited towards elucidating the ideal route of administration and the fate of dendritic cells following injection. Many direct cell labeling approaches utilizing MRI have been attempted for monitoring DC vaccines for immunotherapy. MRI tracking of dendritic cells using super paramagnetic iron oxide (SPIO) nanoparticles has recently been tested in the clinic. In one such study, SPIO-labeled DCs were injected intra-nodally into patients bearing melanoma (*15*). MR imaging was able to detect lymph nodes containing labeled DCs with high sensitivity and revealed several patients who had been mis-injected during therapy. In this case, it is very clear how imaging could help potentially improve therapeutic success rates of patients receiving dendritic cell vaccines.

Applications of immuno-imaging go far beyond the several highlights listed here. In the coming years there will likely be increasing applications of the immuno-imaging toolbox towards autoimmune diseases such as graft versus host disease (*16*) and rheumatoid arthritis, as well as neurodegenerative diseases with an immune component such as multiple sclerosis (*17*) and Alzheimer's.

Part III. The Expanding Roles for Immuno-Imaging

For immunotherapies to succeed, they must make it from the bench to the bedside and lessons learned be brought back to the bench. The standard drug development pipeline usually consists of the following steps: target identification and assessment, lead compound optimization, preclinical studies, clinical phases I-III, and finally, FDA approval. This pipeline represents an approximately 15-year long effort, costing hundreds of millions of dollars, with 1 in 10,000 compounds ultimately achieving success (*18*).

Immuno-imaging has a number of roles to play in the immunotherapy drug development pipeline and could help streamline clinical translation of immunotherapy strategies. During preclinical assessment of cancer immunotherapies, imaging can help guide rationale therapy optimization. Compared to many preclinical drug studies where survival is the primary endpoint, immuno-imaging can give specific insights into the therapeutic mechanisms of action and failure. As we have seen in the examples provided in this review, imaging can elucidate if immune cells are sufficiently homing to the disease site, whether they are activated upon arrival, and how long they viably persist. Based on this information, one can tailor the treatment to overcome specific therapeutic obstacles, rather than taking a random combinatorial approach towards therapeutic optimization. As drugs progress from a company's preclinical pipeline into clinical trials, immuno-imaging has the potential to enable better patient selection/stratification to improve trial design and hopefully outcomes. With the increase in personalized medicine approaches and highly targeted therapeutics (i.e. checkpoint inhibitors), it is critical to see if the patient expresses the drug target prior to administering the drug. Target expression is difficult to capture using any technique besides imaging due to highly heterogeneous expression and spatiotemporal variance. PET imaging lends itself readily to this challenge and can even enable quantitative assessment of target expression, informing not only patient and drug selection but drug dosing as well. Finally, once a drug has received FDA approval, immuno-imaging can serve as a companion diagnostic and monitoring tool for improved patient management. Dynamic changes in immune cell response and checkpoint expression could inform when to take a patient off a certain drug and switch to another, or whether the patient is responding and no longer needs to receive costly therapy. In this way, imaging will enable doctors to make better decisions regarding treatment options and patient follow-up.

For new immuno-imaging techniques to be adopted and succeed in the clinic, the field needs to move towards demonstrating the potential utility of novel probes or biomarkers during preclinical studies. Too often a study concludes with simply validating an immuno-imaging probe as being specific and sensitive. Future studies will need to show that immuno-imaging agents give novel or actionable insights into immune response and therapy. Comparative analyses of immuno-imaging agents being proposed for similar purposes needs to be done and mathematical modeling should be increasingly performed to derive guiding principles for immuno-imaging design and application. The burden still lies on many novel

imaging probes to show that they add additional information to anatomical scans or commonly utilized ^{18}F-FDG PET (*19*). Efforts invested in translating the most promising immuno-imaging agents need to be sped up to keep up with the pace of drug development. Finally, immuno-imaging should not be thought of as a competing tool with blood-based biomarkers or 'Omic' approaches. It is our belief that true success towards understanding and predicting responses to immunotherapy will rely on the integration of the immuno-imaging toolbox with both omics and systems immunology tools. Machine learning and artificial intelligence will be necessary to make sense of the high dimensional data sets acquired across multiple modalities, and these systems will ultimately lead to better clinical decision making and improved patient outcomes. It is clear that the immuno-imaging toolbox will continue to expand and novel imaging strategies will likely play an increasing role in the clinic in years to come.

Review Criteria.

We searched the PubMed database for articles using the terms "immune imaging," "imaging immunotherapy," or "cell tracking." All English-language articles published since 1990 until the date of submission were considered but articles published over the past 5-10 years were given priority. While this review attempts to provide a comprehensive overview of the current-state-of-the-art immuno-imaging toolbox, there have been many applications of the various imaging agents summarized here that were not able to be discussed within the scope of this review.

Acknowledgements.

We would like to thank funding support from the Canary Foundation, Ben & Catherine Ivy Foundation, Sir Peter Michael Foundation, Parker Foundation, and NCI grant funding R01 CA201719 (SSG). We would also like to thank the numerous trainees over the last 20 years in the Gambhir lab to help make several of the strategies discussed in this review possible.

References

1 Slomka PJ, Pan T, Germano G. Recent advances and future progress in PET instrumentation. *Semin Nucl Med*. 2016;46:5–19.

2. De Groeve K, Deschacht N, De Koninck C, et al. Nanobodies as tools for in vivo imaging of specific immune cell types. *J Nucl Med*. 2010;51:782–789.

3. Ngen EJ, Artemov D. Advances in monitoring cell-based therapies with magnetic resonance imaging: future perspectives. *Int J Mol Sci*. 2017;18:14–22.

4. Liao F, Xu H, Torrey N, Road P, Jolla L. In vivo imaging with antibodies and engineered fragments. 2015;2:142–152.

5. Vaneycken I, D'huyvetter M, Hernot S, et al. Immuno-imaging using nanobodies. *Curr Opin Biotechnol*. 2011;22:877–881.

6. Maute RL, Gordon SR, Mayer AT, et al. Engineering high-affinity PD-1 variants for optimized immunotherapy and immuno-PET imaging. *Proc Natl Acad Sci*. 2015;112:6506-14.

7. Wittrup KD, Thurber GM, Schmidt MM, et al. Practical theoretic guidance for the design of tumor-targeting agents. *Methods Enzym*. 2012;503:55-68.

8. Brader P, Serganova I, Blasberg RG. Noninvasive molecular imaging using reporter genes. *J Nucl Med*. 2013;54:167–72.

9. Ehlerding EB, England CG, McNeel DG, Cai W. Molecular imaging of immunotherapy targets in cancer. *J Nucl Med*. 2016;57:1487-1492.

10. Heskamp S, Hobo W, Molkenboer-Kuenen JD, et al. Non-invasive imaging of tumor PD-L1 expression using radiolabeled anti-PD-L1 antibodies. *Cancer Res*. 2015;75:2928-36.

11. Rashidian M, Ingram JR, Dougan M, et al. Predicting the response to CTLA-4 blockade by longitudinal noninvasive monitoring of CD8 T cells. The Journal of Experimental Medicine. 2017;214:2243-2255.

12. Bonifant CL, Jackson HJ, Brentjens RJ, Curran KJ. Toxicity and management in CAR T-cell therapy. *Mol Ther - Oncolytics*. 2016;3:16011.

13. Keu KV, Witney TH, Yaghoubi S, et al. Reporter gene imaging of targeted T cell immunotherapy in recurrent glioma. *Sci Transl Med*. 2017;9.

14. Yaghoubi SS, Jensen MC, Satyamurthy N, et al. Noninvasive detection of therapeutic cytolytic T cells with 18F-FHBG PET in a patient with glioma. *Nat Clin Pract Oncol*. 2009;6:53–58.

15. de Vries IJM, Lesterhuis WJ, Barentsz JO, et al. Magnetic resonance tracking of dendritic cells in melanoma patients for monitoring of cellular therapy. *Nat Biotechnol*. 2005;23:1407–1413.

16. Ronald JA, Kim BS, Gowrishankar G, et al. A PET imaging strategy to visualize activated T cells in acute graft-versus-host disease elicited by allogenic hematopoietic cell transplant. *Cancer Res*. 2017;77:2893–2902.

17. James ML, Hoehne A, Mayer AT, et al. Imaging B cells in a mouse model of multiple sclerosis using ^{64} Cu-Rituximab-PET. *J Nucl Med*. 2017;58:1845-1851.

18. Willmann J, van Bruggen N, Dinkelborg LM, Gambhir SS. Molecular imaging in drug development. *Nat Rev Drug Discov*. 2008;7:591–607.

19. Cho SY, Lipson EJ, Im HJ, et al. Prediction of response to immune checkpoint inhibitor therapy using early time-point FDG-PET/CT imaging in patients with advanced melanoma. *J Nucl Med*. 2017;58:1421-1428.

20. Donnelly DJ, Smith RA, Morin P, et al. Synthesis and biological evaluation of a novel (18)F-labeled adnectin as a PET radioligand for imaging PD-L1 expression. *J Nucl Med.* 2018;59:529-535.

21. Gonzalez Trotter DE, Meng X, McQuade P, et al. In vivo imaging of the programmed death ligand 1 by ^{18}F positron emission tomography. *J Nucl Med*. 2017;58:1852-1857.

22. Maute RL, Gordon SR, Mayer AT, Mccracken MN, Natarajan A, et al. Engineering high-affinity PD-1 variants for optimized immunotherapy and immuno-PET imaging. *Proc Natl Acad Sci.* 2015;112:6506-14.

23. Mayer AT, Natarajan A, Gordon S, et al. Practical ImmunoPET radiotracer design considerations for human immune checkpoint imaging. *J Nucl Med*. 2017;58:538-546.

24. Chatterjee S, Lesniak WG, Nimmagadda S. Noninvasive imaging of immune checkpoint ligand PD-L1 in tumors and metastases for guiding immunotherapy. *Mol Imaging*. 2017;16:15360.

25. Lesniak WG, Chatterjee S, Gabrielson M, et al. PD-L1 Detection in tumors using [64Cu]Atezolizumab with PET. *Bioconjug Chem*. 2016;27:2103–2110.

26. Truillet C, Oh HLJ, Yeo SP, et al. Imaging PD-L1 expression with ImmunoPET. *Bioconjug Chem*. 2018;29:96-103.

27. Heskamp S, Hobo W, Molkenboer-Kuenen JDM, et al. Noninvasive imaging of tumor PD-L1 expression using radiolabeled Anti-PD-L1 antibodies. *Cancer Res*. 2015;75:2928–2936.

28. Josefsson A, Nedrow JR, Park S, et al. Imaging, biodistribution, and dosimetry of radionuclide-labeled PD-L1 antibody in an immunocompetent mouse model of breast cancer. *Cancer Res*. 2016;76:472–479.

29. Nedrow JR, Josefsson A, Park S, et al. Imaging of programmed cell death ligand 1: Impact of protein concentration on distribution of Anti-PD-L1 SPECT agents in an immunocompetent murine model of melanoma. *J Nucl Med*. 2017;58:1560–1566.

30. Kikuchi M, Clump DA, Srivastava RM, et al. Preclinical immunoPET/CT imaging using Zr-89-labeled anti-PD-L1 monoclonal antibody for assessing radiation-induced PD-L1 upregulation in head and neck cancer and melanoma. *Oncoimmunology*. 2017;6:1–13.

31. Meir R, Shamalov K, Sadan T, et al. Fast image-guided stratification using anti-programmed death ligand 1 gold nanoparticles for cancer immunotherapy. *ACS Nano*. 2017;11:11127-11134.

32. Broos K, Keyaerts M, Lecocq Q, et al. Non-invasive assessment of murine PD-L1 levels in syngeneic tumor models by nuclear imaging with nanobody tracers. *Oncotarget*. 2017;8:41932–41946.

33. Chatterjee S, Lesniak WG, Miller MS, et al. Rapid PD-L1 detection in tumors with PET using a highly specific peptide. *Biochem Biophys Res Commun*. 2017;483:258-263.

34. Hettich M, Braun F, Bartholomä MD, Schirmbeck R, Niedermann G. High-resolution PET imaging with therapeutic antibody-based PD-1/PD-L1 checkpoint tracers. *Theranostics*. 2016;6:1629–1640.

35. Ingram JR, Dougan M, Rashidian M, et al. PD-L1 is an activation-independent marker of brown adipocytes. *Nat Commun*. 2017;8:647.

36. England CG, Ehlerding EB, Hernandez R, et al. Preclinical parmacokinetics and biodistribution studies of Zr-labeled Pembrolizumab. *J Nucl Med*. 2016;4116:1–22.

37. England CG, Jiang D, Ehlerding EB, et al. 89Zr-labeled Nivolumab for imaging of T-cell infiltration in a humanized murine model of lung cancer. *Eur J Nucl Med Mol Imaging*. 2017;2:1–11.

38. Natarajan A, Mayer AT, Reeves RE, Nagamine CM, Gambhir SS. Development of novel ImmunoPET tracers to image human PD-1 checkpoint expression on tumor-infiltrating lymphocytes in a humanized mouse model. *Mol Imaging Biol*. 2017;19:903–914.

39. Du Y, Liang X, Li Y, et al. Nuclear and fluorescent labeled PD-1-Liposome-DOX- ^{64} Cu/IRDye800CW allows improved breast tumor targeted imaging and therapy. *Mol Pharm*. 2017;14:3978-3986.

40. Natarajan A, Mayer AT, Xu L, et al. A novel radiotracer for immunoPET imaging of PD-1 checkpoint expression on tumor infiltrating lymphocytes. *Bioconjug Chem*. 2015;26:2602-9.

41. Yusufi N, Mall S, Bianchi H de O, et al. In-depth characterization of a TCR-specific tracer for sensitive detection of tumor-directed transgenic T cells by immuno-PET. *Theranostics*. 2017;7:2402–2416.

42. Mall S, Yusufi N, Wagner R, et al. Immuno-PET imaging of engineered human T cells in tumors. *Cancer Res*. 2016;76:4113–4123.

43. Griessinger CM, Maurer A, Kesenheimer C, et al. ^{64} Cu antibody-targeting of the T-cell receptor and subsequent internalization enables in vivo tracking of lymphocytes by PET. *Proc Natl Acad Sci*. 2015;112:1161–1166.

44. Rashidian M, Keliher EJ, Bilate AM, et al. Noninvasive imaging of immune responses. *Proc Natl Acad Sci*. 2015;112:6146-51.

45. Van Elssen C, Rashidian M, Vrbanac V, et al. Noninvasive imaging of human immune responses in a human xenograft model of graft- versus-host disease. *J Nucl Med*. 2017;58:1003-1008.

46. Larimer BM, Wehrenberg-Klee E, Dubois F, et al. Granzyme B PET imaging as a predictive biomarker of immunotherapy response. *Cancer Res*. 2017;77:2318–2327.

47. Higashikawa K, Yagi K, Watanabe K, et al. 64Cu-DOTA-anti-CTLA-4 mAb enabled PET visualization of CTLA-4 on the T-cell infiltrating tumor tissues. *PLoS One*. 2014;9.

48. Ehlerding EB, England CG, Majewski RL, et al. ImmunoPET imaging of CTLA-4 expression in mouse models of non-small cell lung cancer. *Mol Pharm*. 2017;14:1782–1789.

49. Tavaré R, Escuin-Ordinas H, Mok S, et al. An effective immuno-PET imaging method to monitor CD8-dependent responses to immunotherapy. *Cancer Res*. 2016;76:73–82.

50. Tavaré R, McCracken MN, Zettlitz KA, et al. Engineered antibody fragments for immuno-PET imaging of endogenous CD8+ T cells in vivo. *Proc Natl Acad Sci U S A*. 2014;111:1108–13.

51. Olafsen T, Torgov M, Zhang GG, et al. Pet imaging of cytotoxic human T cells using an 89Zr-labeled anti-CD8 minibody. *J Immunother Cancer*. 2015;3:388.

52. Tavaré R, Mccracken MN, Zettlitz KA, et al. Immuno-PET of murine T cell reconstitution postadoptive stem cell transplantation using anti-CD4 and anti-CD8 cys-diabodies. *J Nucl Med.* 2015;56:1258-64.

53. Freise AC, Zettlitz KA, Salazar FB, et al. ImmunoPET imaging of murine CD4+ T cells using anti-CD4 cys-diabody: effects of protein dose on T cell function and imaging. *Mol Imaging Biol*. 2017;19:599-609.

54. Larimer BM, Wehrenberg-Klee E, Caraballo A, Mahmood U. Quantitative CD3 PET imaging predicts tumor growth response to anti-CTLA-4 therapy. *J Nucl Med*. 2016;57:1607–1611.

55. Hartimath SV, Draghiciu O, van de Wall S, et al. Noninvasive monitoring of cancer therapy induced activated T cells using [^{18} F]FB-IL-2 PET imaging. *Oncoimmunology*. 2016;6:1248014.

56. Glaudemans AWJM, Bonanno E, Galli F, et al. In vivo and in vitro evidence that 99mTc-HYNIC-

interleukin-2 is able to detect T lymphocytes in vulnerable atherosclerotic plaques of the carotid artery. *Eur J Nucl Med Mol Imaging*. 2014;41:1710–9.

57. Olafsen T, Sirk SJ, Betting DJ, et al. ImmunoPET imaging of B-cell lymphoma using 124I-anti-CD20 scFv dimers (diabodies). *Protein Eng Des Sel*. 2010;23:243–249.

58. Zettlitz KA, Tavare R, Knowles SM, et al. ImmunoPET of malignant and normal B cells with ^{89}Zr- and ^{124}I-labeled obinutuzumab antibody fragments reveals differential CD20 internalization in vivo. *Clin Cancer Res*. 2017;23:7242-7252.

59. Natarajan A, Hackel BJ, Gambhir SS. A novel engineered anti-CD20 tracer enables early time PET imaging in a humanized transgenic mouse model of B-cell non-hodgkins lymphoma. *Clin Cancer Res*. 2013;19:6820–6829.

60. Natarajan A, Habte F, Gambhir SS. Development of a novel long-lived immunoPET tracer for monitoring lymphoma therapy in a humanized transgenic mouse model. *Bioconjug Chem*. 2012;23:1221–1229.

61. Natarajan A, Gambhir SS. Radiation dosimetry study of [89Zr]Rituximab tracer for clinical translation of B cell NHL imaging using Positron Emission Tomography. *Mol Imaging Biol*. 2015;17:539-47

62. Walther M, Gebhardt P, Grosse-Gehling P, et al. Implementation of 89Zr production and in vivo imaging of B-cells in mice with 89Zr-labeled anti-B-cell antibodies by small animal PET/CT. *Appl Radiat Isot*. 2011;69:852–857.

63. Olafsen T, Betting D, Kenanova VE, et al. Recombinant anti-CD20 antibody fragments for small-animal PET imaging of B-cell lymphomas. *J Nucl Med*. 2009;50:1500–1508.

64. Radu CG. Shu CJ, Nair-Gill E, et al. Molecular imaging of lymphoid organs and immune activation by positron emission tomography with a new [18 F]-labeled 2-deoxycytidine analog. *Nat Med*. 2008;14:783–788.

65. Kim W, Le TM, Wei L, et al. [18F]CFA as a clinically translatable probe for PET imaging of deoxycytidine kinase activity. *Proc Natl Acad Sci*. 2016;113:4027-32.

66. Namavari M, Chang YF, Kusler B, et al. Synthesis of 2'-Deoxy-2'-[18F]fluoro-9- D-Arabinofuranosylguanine: A novel agent for imaging T-cell activation with PET. *Mol Imaging Biol*. 2011;13:812–818.

67. Ribas A, Benz MR, Allen-Auerbach MS, et al. Imaging of CTLA4 blockade-induced cell replication with 18F-FLT PET in patients with advanced melanoma treated with Tremelimumab. *J Nucl Med*. 2010;51:340–346.

68. Zheleznyak A, Ikotun OF, Dimitry J, Frazier WA, Lapi SE. Imaging of CD47 expression in xenograft and allograft tumor models. *Mol Imaging*. 2013;12:1–10.

69. Bachawal SV, Jensen KC, Wilson KE, et al. Breast cancer detection by B7-H3-targeted ultrasound molecular imaging. *Cancer Res*. 2015;75:2501–2509.

70. Nimmagadda S, Pullambhatla M, Stone K, et al. Molecular imaging of CXCR4 receptor expression in human cancer xenografts with [64Cu]AMD3100 positron emission tomography. *Cancer Res*. 2010;70:3935–3944.

71. Blykers A, Schoonooghe S, Xavier C, et al. PET imaging of macrophage mannose receptor-expressing macrophages in tumor stroma using 18F-radiolabeled camelid single-domain antibody fragments. *J Nucl Med*. 2015;56:1265–1271.

72. Sagiv-Barfi I, Czerwinski DK, Levy S, et al. Eradication of spontaneous malignancy by local immunotherapy. *Sci Transl Med*. 2018;10.

73. Alam IS, Mayer AT, Sagiv-Barfi I, et al. Imaging activated T cells predicts response to cancer vaccines. *J Clin Invest*. 2018;128.

74. Botti C, Negri DRM, Seregni E, et al. Comparison of three different methods for radiolabelling human activated T lymphocytes. *Eur J Nucl Med*. 1997;24:497–504.

75. Pittet MJ, Grimm J, Berger CR, et al. In vivo imaging of T cell delivery to tumors after adoptive transfer therapy. *Proc Natl Acad Sci U S A*. 2007;104:12457–12461.

76. Kircher MF, Allport JR, et al. In vivo high resolution three-dimensional imaging of antigen-specific cytotoxic T-lymphocyte trafficking to tumors. *Cancer Res*. 2003;63:6838--6846.

77. Zanzonico P, Koehne G, Gallardo HF, et al. [131I]FIAU labeling of genetically transduced, tumor-reactive lymphocytes: cell-level dosimetry and dose-dependent toxicity. *Eur J Nucl Med Mol Imaging*. 2006;33:988–997.

78. Liu L, Ye Q, Wu Y, et al. Tracking T-cells in vivo with a new nano-sized MRI contrast agent. *Nanomedicine Nanotechnology, Biol Med*. 2012;8:1345–1354.

79. Srinivas M, Morel PA, Ernst LA, Laidlaw DH, Ahrens ET. Fluorine-19 MRI for visualization and quantification of cell migration in a diabetes model. *Magn Reson Med*. 2007;58:725–734.

80. Bhatnagar P, Alauddin M, Bankson JA, et al. Tumor lysing genetically engineered T cells loaded with multi-modal imaging agents. *Sci Rep*. 2014;4:1–6.

81. Youniss FM, Sundaresan G, Graham LJ, et al. Near-infrared imaging of adoptive immune cell therapy in breast cancer model using cell membrane labeling. *PLoS One*. 2014;9:1–10.

82. Koehne G, Doubrovin M, Doubrovina E, et al. Serial in vivo imaging of the targeted migration of human HSV-TK-transduced antigen-specific lymphocytes. *Nat Biotechnol*. 2003;21:405–413.

83. Chewning JH, Dugger KJ, Chaudhuri TR, Zinn KR, Weaver CT. Bioluminescence-based visualization of CD4 T cell dynamics using a T lineage-specific luciferase transgenic model. *BMC Immunol*. 2009;10.

84. Kim H, Peng G, Hicks JM, et al. Engineering human tumor-specific cytotoxic T cells to function in a hypoxic environment. *Mol Ther*. 2008;16:599–606.

85. Shu CJ, Radu CG, Shelly SM, et al. Quantitative PET reporter gene imaging of CD8+T cells specific for a melanoma-expressed self-antigen. *Int Immunol*. 2009;21:155–165.

86. Dotti G, Tian M, Savoldo B, et al. Repetitive noninvasive monitoring of HSV1-tk-expressing T cells intravenously infused into nonhuman primates using positron emission tomogrpahy and computed tomography with 18F-FEAU. *Mol Imaging.* 2011;8:230–237.

87. Thorek DLJ, Tsao PY, Arora V, et al. In vivo, multimodal imaging of B cell distribution and response to antibody immunotherapy in mice. *PLoS One*. 2010;5.

88. Paik JY, Lee KH, Byun SS, Choe YS, Kim BT. Use of insulin to improve [18 F]fluorodeoxyglucose labelling and retention for in vivo positron emission tomography imaging of monocyte trafficking. *Nucl Med Commun*. 2002;23:551–7.

89. Kang S, Lee HW, Jeon YH, et al. Combined cluorescence and magnetic resonance imaging of primary macrophage migration to sites of acute inflammation using near-infrared fluorescent magnetic nanoparticles. *Mol Imaging Biol*. 2015;17:643–651.

90. Gramoun A, Crowe LA, Maurizi L, et al. Monitoring the effects of dexamethasone treatment by MRI using in vivo iron oxide nanoparticle-labeled macrophages. *Arthritis Res Ther*. 2014;16:131.

91. Daldrup-Link HE, Golovko D, Ruffell B, et al. MRI of tumor-associated macrophages with clinically applicable iron oxide nanoparticles. *Clin Cancer Res*. 2011;17:5695–5704.

92. Yang CY, Tai MF, Lin CP, et al. Mechanism of cellular uptake and impact of ferucarbotran on macrophage physiology. *PLoS One*. 2011;6:1–7.

93. Raynal I, Prigent P, Peyramaure S, et al. Macrophage endocytosis of superparamagnetic iron oxide nanoparticles: mechanisms and comparison of ferumoxides and ferumoxtran-10. *Invest Radiol*. 2004;39:56–63.

94. Kirschbaum K, Sonner JK, Zeller MW, et al. In vivo nanoparticle imaging of innate immune cells can serve as a marker of disease severity in a model of multiple sclerosis. *Proc Natl Acad Sci*. 2016;113(46):13227-13232.

95. Keliher EJ, Yoo J, Nahrendorf M, et al. 89Zr-labeled dextran nanoparticles allow in vivo macrophage imaging. *Bioconjug Chem.* 2012;22:2383–2389.

96. Lee HW, Jeon YH, Hwang MH, et al. Dual reporter gene imaging for tracking macrophage migration using the human sodium iodide symporter and an enhanced firefly luciferase in a murine inflammation model. *Mol Imaging Biol*. 2013;15:703–712.

97. Choi YJ, Oh SG, Singh TD, et al. Visualization of the biological behavior of tumor-associated macrophages in living mice with colon cancer using multimodal optical reporter gene imaging. *Neoplasia*. 2016;18:133–141.

98. Seo JH, Jeon YH, Lee YJ, et al. Trafficking macrophage migration using reporter gene imaging with human sodium iodide symporter in animal models of inflammation. *J Nucl Med*. 2010;51:1637–1643.

99. Ridolfi R, Riccobon A, Galassi R, et al. Evaluation of in vivo labelled dendritic cell migration in cancer patients. *J Transl Med*. 2004;2:1–11.

100. De Vries IJM, Krooshoop DJEB, Scharenborg NM, et al. Effective migration of antigen-pulsed dendritic cells to lymph nodes in melanoma patients is determined by their maturation state. *Cancer Res*. 2003;1:12–17.

101. Ahrens ET, Flores R, Xu H, Morel PA. In vivo imaging platform for tracking immunotherapeutic cells. *Nat Biotechnol*. 2005;23:983–987.

102. Baumjohann D, Hess A, Budinsky L, et al. In vivo magnetic resonance imaging of dendritic cell migration into the draining lymph nodes of mice. *Eur J Immunol*. 2006;36:2544–2555.

103. Noh Y-W, Lim YT, Chung BH. Noninvasive imaging of dendritic cell migration into lymph nodes using near-infrared fluorescent semiconductor nanocrystals. *FASEB J*. 2008;22:3908–3918.

104. Olasz EB, Lang L, Seidel J, et al. Fluorine-18 labeled mouse bone marrow-derived dendritic cells can be detected in vivo by high resolution projection imaging. *J Immunol Methods*. 2002;260:137–148.

105. Ahrens ET, Helfer BM, O'Hanlon CF, Schirda C. Clinical cell therapy imaging using a perfluorocarbon tracer and fluorine-19 MRI. *Magn Reson Med*. 2014;72:1696–1701.

106. Stoll S, Delon J, Tilmann BM, Germain RN. Dynamic imaging of T cell – dendritic cell interactions in lymph nodes. *Science*. 2002;296:1873–1877.

107. Lee HW, Yoon SY, Singh TD, et al. Tracking of dendritic cell migration into lymph nodes using molecular imaging with sodium iodide symporter and enhanced firefly luciferase genes. *Sci Rep*. 2015;5:9865.

108. Kim HS, Woo J, Lee JH, et al. In vivo tracking of dendritic cell using MRI reporter gene, ferritin. *PLoS One*. 2015;10:1–13.

109. Schimmelpfennig CH, Schulz S, Arber C, et al. Ex vivo expanded dendritic cells home to T-cell zones of lymphoid organs and survive in vivo after allogeneic bone marrow transplantation. *Am J*

Pathol. 2005;167:1321–1331.

110. Daldrup-Link HE, Meier R, Rudelius M, et al. In vivo tracking of genetically engineered, anti-HER2/neu directed natural killer cells to HER2/neu positive mammary tumors with magnetic resonance imaging. *Eur Radiol*. 2005;15:4–13.

111. Tavri S, Jha P, Meier R, et al. Optical imaging of cellular immunotherapy against prostate cancer. *Mol Imaging*. 2009;8:15–26.

112. Melder RJ, Brownell AL, Shoup TM, Brownell GL, Jain RK. Imaging of activated natural killer cells in mice by positron emission tomography : preferential uptake in tumors. *Cancer Res.* 1993;5867–5871.

113. Meller B, Frohn C, Brand JM, et al. Monitoring of a new approach of immunotherapy with allogenic (111)In-labelled NK cells in patients with renal cell carcinoma. *Eur J Nucl Med Mol Imaging*. 2004;31:403–407.

114. Kurtz DM, Gambhir SS. Tracking cellular and immune therapies in cancer. *Adv Cancer Res*. 2014;124:257-96.

115. Chatterjee S, Lesniak WG, Gabrielson M, et al. A humanized antibody for imaging immune checkpoint ligand PD-L1 expression in tumors. *Oncotarget*. 2016;7:10215–10227.

116. Arlauckas SP, Garris CS, Kohler RH, et al. In vivo imaging reveals a tumor-associated macrophage–mediated resistance pathway in anti–PD-1 therapy. *Sci Transl Med*. 2017;9:3604.

A Probes targeted for endogenous immune cell biomarkers

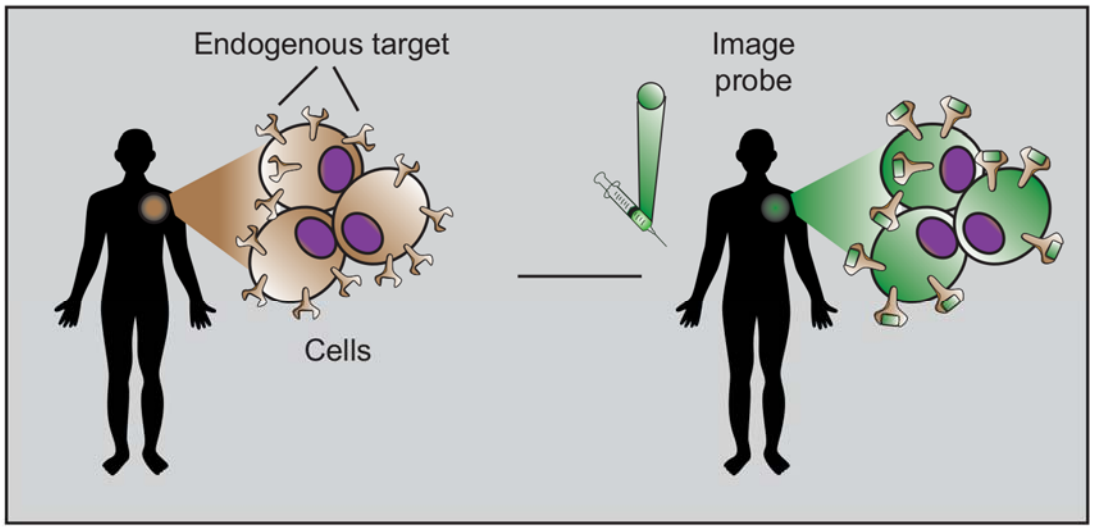

B Indirect immune cell labeling strategies

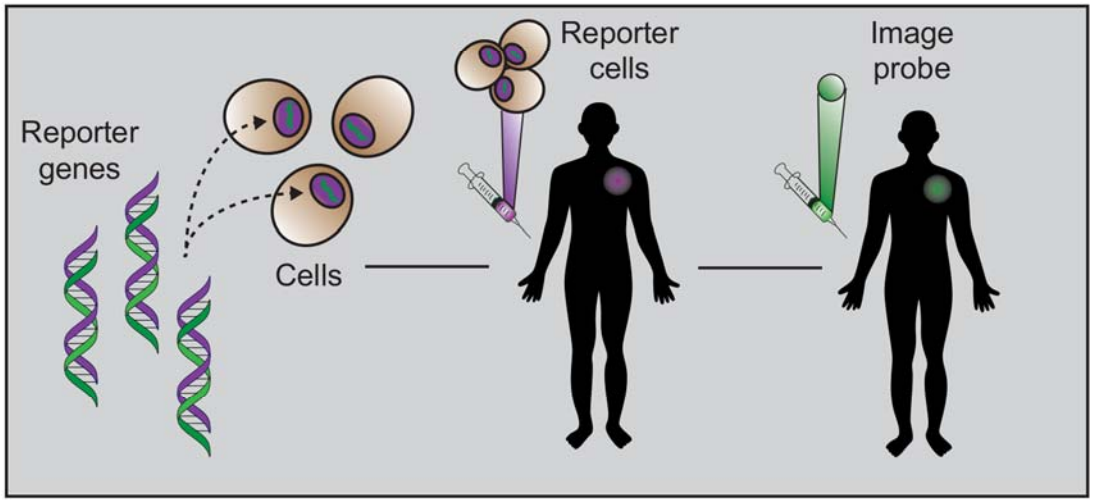

C Direct immune cell labeling strategies

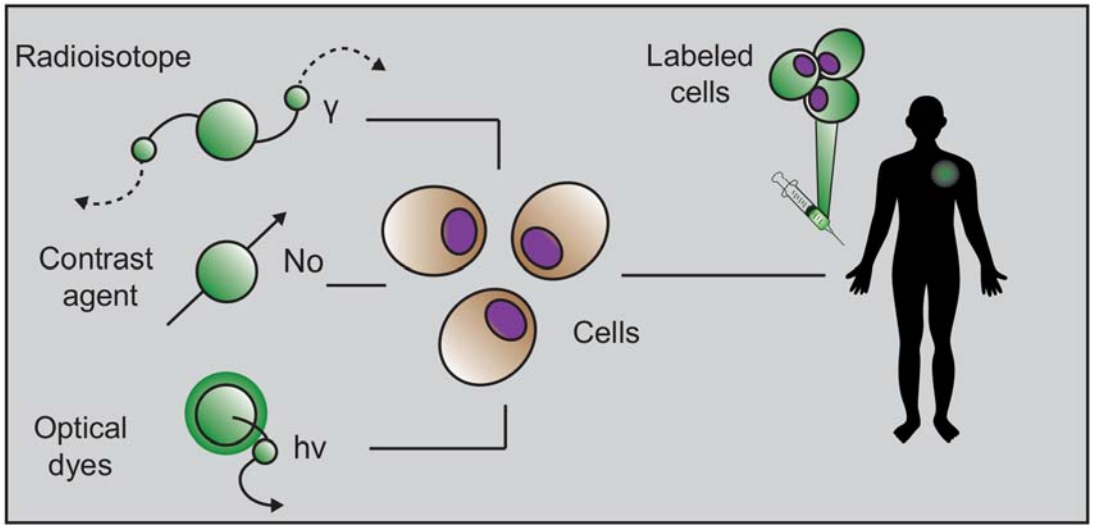

Figure 1. ***Immuno-Imaging Strategies.*** Adapted from Kurtz et al (*114*). Schematic representation of the three primary strategies utilized for imaging immune cells. **a)** Probes targeted for endogenous immune cell biomarkers. Here, an imaging probe is injected targeting a natural immune cell receptor. **b)** Indirect immune cell labeling strategies. In this strategy, cells removed from a patient are transduced with a reporter gene and reinjected. Cells are then visualized via the injection of a reporter probe. **c)** Direct immune cell labeling strategies. Here, cells taken from a patient's own body are incubated ex vivo with an imaging probe. The labeled cells are injected into the patient and monitored via imaging.

A Immune checkpoint blockade

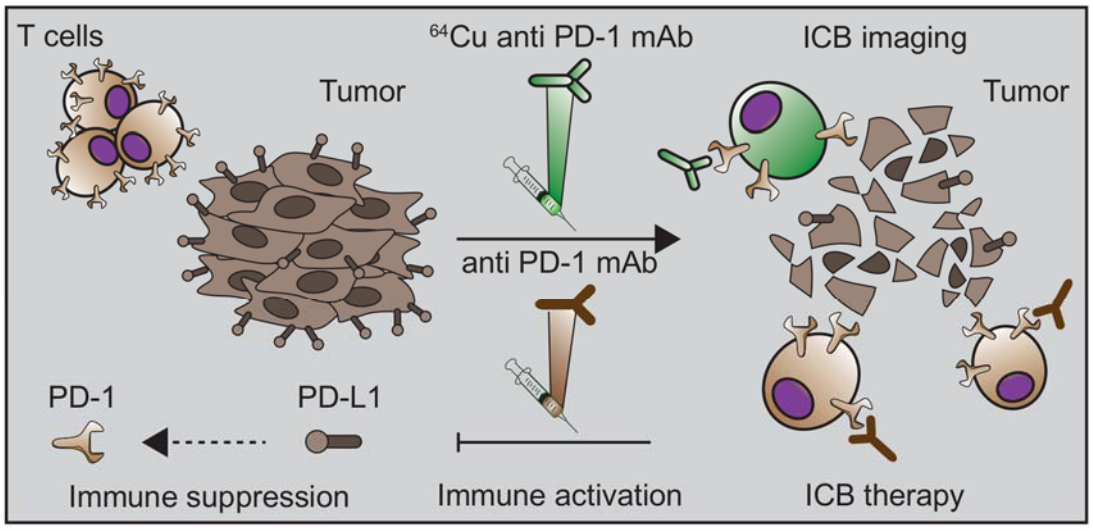

B Chimeric antigen receptor T cell therapy

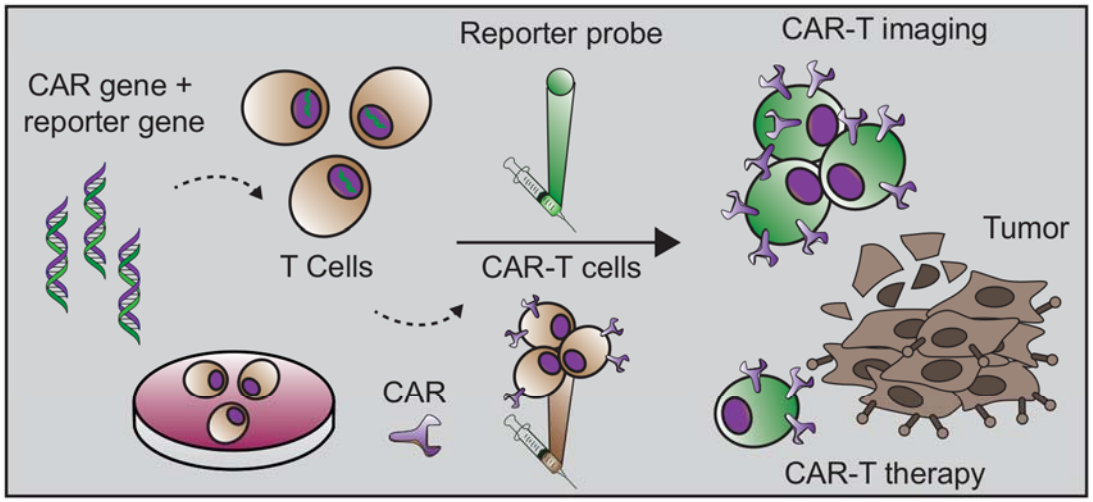

C Dendritic cell vaccines

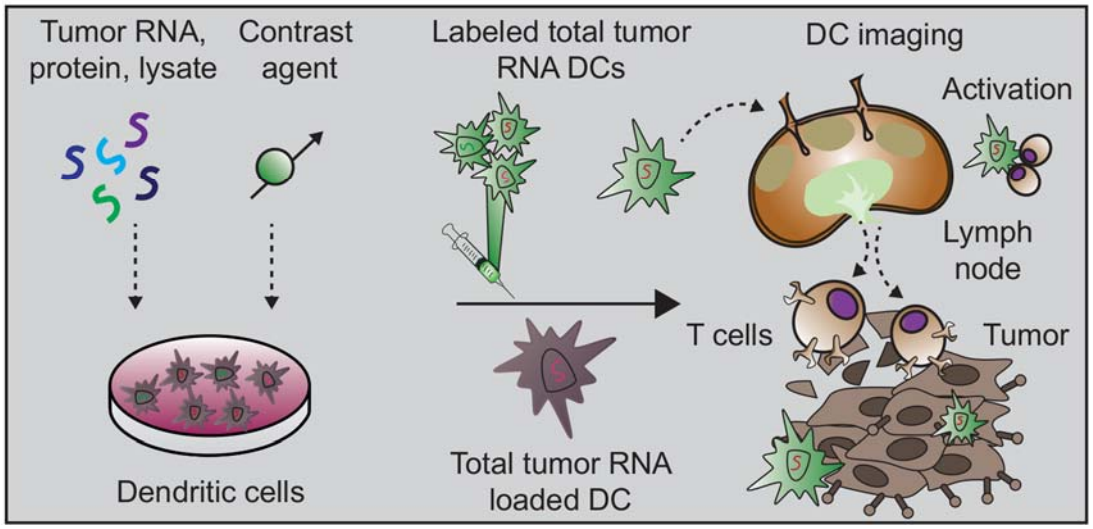

Figure 2. ***Immuno-Imaging Applications Towards Immunotherapy.*** Immune checkpoint blockade, CAR-Ts, and therapeutic vaccines constitute three important classes of cancer immunotherapy. **a)** Immune checkpoints that regulate anti-tumor immunity have now been identified as promising therapeutic targets. Blocking signaling pathways that suppress anti-tumor immune responses has proven especially effective. In one approach, an anti-PD-1 mAb targets the PD-1 receptor on T cells, blocking ligation of the receptor and immunosuppression by PD-L1 on tumor cells. Anti-PD1 mAb administration thus leads to immune activation and therapeutic response. Imaging the expression of PD1 with a radiolabeled mAb may assist in selection of patients for treatment, optimal dosing and response monitoring. **b)** CAR-T strategies engineer a patient's immune cells ex vivo to express a receptor that can bind specifically to tumor cells. During this engineering process a reporter gene can also be inserted to enable longitudinal tracking of the CAR-T cells. Upon administration, CAR-Ts seek out and destroy malignant tumor cells. Subsequent imaging with a reporter probe can give insights into their location and functional status. **c)** Cancer vaccine strategies come in many formulations. In one approach, dendritic cells are pulsed with tumor antigen, lysate or RNA. Dendritic cells then express tumor antigens on their MHC molecules, which are capable of eliciting a T cell driven immune response. Successful responses require homing of dendritic cells to the lymph nodes and tumor. At these sites the dendritic cells are capable of activating tumor specific T cells. Labeling the dendritic cells with a contrast agent allows for assessment of successful homing of dendritic cells to lymph nodes and other secondary lymphoid sites. This knowledge can be utilized to inform both dose and route of vaccine administration.

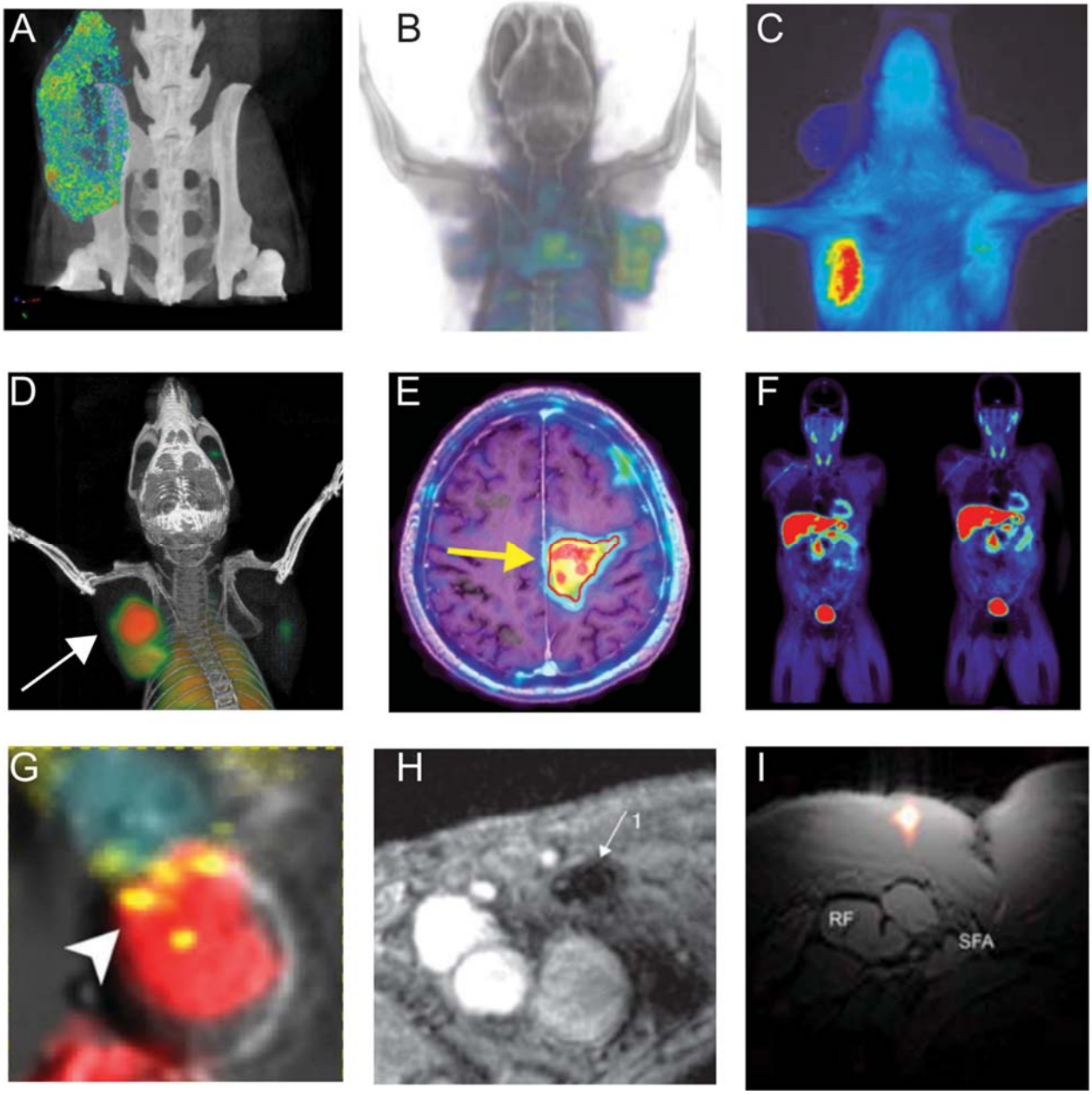

Figure 3. *Immuno-Imaging Examples.* a-c) *Imaging the PD-L1 immune checkpoint.* a) CT imaging using anti-PD-L1 gold nanoparticles; adapted from Meir et al (*31*). b) PET and c) optical imaging of a humanized antibody for assessing PD-L1 expression in tumors; adapted from Chatterjee et al (*115*). **d-f)** *Imaging activated T cells.* d) PET imaging of OX40 expressed on activated T cells following an intratumoral cancer vaccine; adapted from Alam et al (*72*,*73*). Arrow indicates vaccine treated tumor. e) Reporter gene imaging of targeted T cell immunotherapy in recurrent glioma; adapted from Keu et al (*13*). Arrow indicates lesion. f) PET imaging of ^{18}F-AraG to visualize activated T cells in acute graft versus host

disease; adapted from Ronald et al (*16*). **g-i)** *Imaging myeloid cells.* g) Optical imaging reveals a tumor associated macrophage mediated mechanism of resistance to anti-PD1 therapy; adapted from Arlauckas et al (*116*). Macrophage – red, T cell – blue, PD-1 – yellow h) MRI imaging of dendritic cells labeled with SPIO; adapted from de Vries et al (*15*). Arrow indicates site of decreased signal in lymph node due to SPIO labeled dendritic cell accumulation. i) Axial composite $^{19}F/^{1}H$ MRI images following intradermal DC administration into quadriceps of patients; adapted from Ahrens et al (*105*).

Table 1. Probes Targeted for Endogenous Immune Cell Biomarkers

Target	Agents	Class	Reactivity	Modality	Stage	Refs
PD-L1	18F-BMS-986192	Adnectin	Human/Cynomolgus	PET	Preclinical	(*20*)
	18F-NOTA-ZPDL1_1	Affibody	Human/Macaque	PET	Preclinical	(*21*)
	64Cu-DOTA-HAC-PD1, 64Cu-NOTA-HAC-PD1, 64Cu-NOTA-HACA-PD1, 68Ga-NOTA-HAC-PD1, 68Ga-NOTA-HACA- PD1 and 68Ga-DOTA-HACA-PD1	HAC-PD1	Human	PET	Preclinical	(*22*, *23*)
	111IN-Atezolizumab, NIR-Atezolizumab, 64Cu-Atezolizumab, 89Zr-Atezolizumab	Humanized IgG1	Human	SPECT, PET, Optical	**Clinical**	(*24*, *25*)
	89Zr-C4	Humanized IgG1	Human/Murine	PET	Preclinical	(*26*)
	111IN-PD-L1.3.1	Murine IgG1	Human	SPECT	Preclinical	(*27*)
	111IN-DTPA-anti-PDL1	mAb	Murine	SPECT	Preclinical	(28,*29*)
	Zr89-DFO-anti-PDL1	mAb	Murine	PET	Preclinical	(*30*)
	aPDL1-GNPs	Nanoparticle	Murine	CT	Preclinical	(*31*)
	99mTc-Nbs	Nanobody	Murine	SPECT	Preclinical	(*32*)
	64Cu-WL12	Peptide	Human	PET	Preclinical	(*33*)
	64Cu-NOTA-PD-L1	mAb	Murine	PET	Preclinical	(*34*)
	18F-B3, 64Cu-B3	Camelid VhH	Murine	PET	Preclinical	(*35*)
PD-1	89Zr-Df-Pembrolizumab	Humanized IgG4	Human	PET	Preclinical	(*36*)
	89Zr-Df-Nivolumab	Humanized IgG4	Human	PET	Preclinical	(*37*)
	89Zr-Keytruda	Humanized IgG4	Human	PET	Preclinical	(*38*)
	PD-1-Liposome-DOX-64Cu/IRDye800CW	Rat IgG2a	Murine	NIRF/PET	Preclinical	(*39*)
	64Cu-NOTA-PD-1	mAb	Murine	PET	Preclinical	(*34*)
	64Cu-DOTA-anti-PD-1	mAb	Murine	PET	Preclinical	(*40*)
TCR	89Zr-Df-aTCRmu-F(ab')2	Fab'2	Human	PET	Preclinical	(*41*, *42*)
	64Cu-DOTA-KJ1-26	mAb	Murine	PET	Preclinical	(*43*)
MHCI/II	18F-VHH7, 18F-VHHDC13	Camelid VhH	Murine	PET	Preclinical	(*44*)
	64Cu-VHH4	Camelid VhH	Human	PET	Preclinical	(*45*)
Granz B	68Ga-NOTA-GZP	Peptide	Murine	PET	Preclinical	(*46*)
CTLA-4	64Cu-DOTA-anti-CTLA-4	mAb	Murine	PET	Preclinical	(*47*)

	64Cu-DOTA-Ipilimumab	mAb	Human	PET	Preclinical	(*48*)
CD8	89Zr-VHH-X18	Camelid VHH	Murine	PET	Preclinical	(*11*)
	89Zr-malDFO-169cDb	Cys-Diabody	Murine	PET	Preclinical	(*49*)
	64Cu-NOTA-2.43Mb	Minibody	Murine	PET	Preclinical	(*50*)
	89Zr-Df-IAB22M2C	Minibody	Human	PET	**Clinical**	(*51*)
CD4	89Zr-malDFO-GK1.5cDb	Cys-Diabody	Murine	PET	Preclinical	(*52*, *53*)
CD3	89Zr-DFO-CD3	mAb	Murine	PET	Preclinical	(*54*)
CD25	18F-FB-IL2	Wt IL2	Murine	PET	Preclinical	(*55*)
	99Tc-IL2	Wt IL2	Human	SPECT	**Clinical**	(*56*)
CD20	124I-anti-CD20 scFV dimers	Diabody	Human	PET	Preclinical	(*57*)
	64Cu-Rituximab	mAb	Human	PET	Preclinical	(*17*)
	124I-GAcDb, 124I-GAcMb, 89Zr-GAcDb,	Cys-Diabody, Cys-Minibody	Human	PET	Preclinical	(*58*)
	64Cu-FN3CD20	Fibronectin (FNIII)	Human	PET	Preclinical	(*59*)
	89Zr-Df-Bz-Rituximab	mAb	Human	PET	Preclinical	(*60*, *61*)
	89Zr-anti-B220	mAb	Murine	PET	Preclinical	(*62*)
	124I-scFV-Fc DM, 124I-Mb, 64Cu-DOTA-Mb	Minibody, ScFv	Human	PET	Preclinical	(*63*)
dCK	18F-FAC, 18F-CFA	Small Molecule	Murine/Human	PET	**Clinical**	(*64*, *65*)
dGK	18F-AraG	Small Molecule	Murine/Human	PET	**Clinical**	(*16*, *66*)
TK1	18F-FLT	Small Molecule	Murine/Human	PET	**Clinical**	(*67*)
CD47	89Zr-antiCD47-mAb	mAb	Murine/Human	PET	Preclinical	(*68*)
CD276	Anti-B7H3-microbubbles	Microbubble	Human	Ultrasound	Preclinical	(*69*)
CXCR4	64Cu-AMD3100	mAb	Human	PET	Preclinical	(*70*)
MMR	18F-SFB	Nanobody	Murine	PET	**Clinical**	(*71*)
OX40	64Cu-DOTA-OX40	mAb	Murine	PET	Preclinical	(*72*, *73*)

Table 2. Immune Cell Labeling Strategies

Target	Agents	Class	Reactivity	Modality	Stage	Refs
T cells	64Cu-PTSM	Small Molecule	Murine/Human	PET	Preclinical	(*74*)
	18F-FDG	Small Molecule	Murine/Human	PET	Preclinical	(*74*)
	99mTC-MHPAO	Small Molecule	Murine/Human	SPECT	Preclinical	(*74*)
	111In-Oxine	Small Molecule	Murine/Human	SPECT	Preclinical	(*75*)
	CLIO-HD	Nanoparticle	Murine/Human	MRI	Preclinical	(*76*)
	I124-FIAU	Reporter Gene	Murine/Human	PET	**Clinical**	(*77*)
	18F-FHBG	Reporter Gene	Murine/Human	PET	**Clinical**	(*13*)
	IOPC-NH2	Nanoparticle	Murine/Human	MRI	Preclinical	(*78*)
	PFPE/19F	Nanoparticle	Murine/Human	MRI	**Clinical**	(*79*)
	64Cu-SPION	Nanoparticle	Murine/Human	PET	Preclinical	(*80*)
	DiR Fluorophore	Small Molecule	Murine/Human	FLI	Preclinical	(*81*)
	HSVI-sr39tk, HSV-tk,HSV-tk-GFP	Reporter Gene	Murine/Human	PET/Optical	**Clinical**	(*82*)
	Fluc	Reporter Gene	Murine/Human	BLI	Preclinical	(*83*, *84*)
	Sr39tk/F18-FHBG	Reporter Gene	Murine/Human	PET	Preclinical	(*85*)
	18F-FEAU	Reporter Gene	Murine/Human	PET	Preclinical	(*86*)
B Cells	NIR nanoparticle	Nanoparticle	Murine/Human	FLI	Preclinical	(*87*)
Monocytes	18F-FDG	Small Molecule	Murine/Human	PET	**Clinical**	(*88*)
Macrophage	NIR Nanoparticle	Nanoparticle	Murine/Human	FLI	Preclinical	(*89*)
	Ferumoxytol SPIO	Nanoparticle	Murine/Human	MRI	**Clinical**	(*90*, *91*)
	Magnetic NP	Nanoparticle	Murine/Human	MRI	**Clinical**	(*89*)
	Ferucarbotran	Nanoparticle	Murine/Human	MRI	**Clinical**-Discontinued	(*92*)
	Ferumoxstran	Nanoparticle	Murine/Human	MRI	**Clinical**-Discontinued	(*93*)
	CLIO	Nanoparticle	Murine/Human	MRI	Preclinical	(*94*)
	Zr89/64Cu/18F-DNP	Nanoparticle	Mouse	PET	Preclinical	(*95*)
	Fluc	Reporter Gene	Murine/Human	BLI	Preclinical	(*96*, *97*)
	NIS/124I	Reporter Gene	Murine/Human	PET	**Clinical**	(*96*, *98*)
DC	111Indium/99mTc-HMPAO	Small Molecule	Murine/Human	SPECT	**Clinical**	(*99*)
	111Indium	Small Molecule	Murine/Human	SPECT	**Clinical**	(*100*)

	[19F] PFPE loaded w/ iron particles*	Nanoparticle	Murine/Human	MRI	Preclinical	(*101*)
	SPIO	Nanoparticle	Murine/Human	MRI	**Clinical**	(*102*)
	NIR-QD	Quantum Dot	Murine/Human	FLI	Preclinical	(*103*)
	18F-SFB	Small Molecule	Murine/Human	PET	**Clinical**	(*104*)
	Ferumoxide	Nanoparticle	Murine/Human	MRI	**Clinical**	(*15*)
	Perfluorocarbon NP	Nanoparticle	Murine/Human	MRI	**Clinical**	(*105*)
	CFSE	Small Molecule	Murine/Human	FLI	Preclinical	(*106*)
	Fluc	Reporter Gene	Murine/Human	BLI	Preclinical	(*107*)
	hNIS/124I	Reporter Gene	Murine/Human	PET	**Clinical**	(*107*)
	FTH	Reporter Gene	Murine/Human	MRI	**Clinical**	(*108*)
	GFP	Reporter Gene	Murine/Human	FLI	Preclinical	(*109*)
NK Cells	Ferumoxides, Ferucarbon	Nanoparticle	Murine/Human	MRI	Preclinical	(*110*)
	NIR Dye	Small Molecule	Murine/Human	FLI	Preclinical	(*111*)
	11C	Small Molecule	Murine/Human	PET	**Clinical**	(*112*)
	111Indium	Small Molecule	Murine/Human	SPECT	**Clinical**	(*113*)

Table Legend

Common Acronyms. ***Modality*** – PET, positron emission tomography; SPECT, single photon emission computed tomography; FLI, fluorescence imaging; MRI, magnetic resonance imaging; CT, computed tomography; BLI, bioluminescence imaging; NIRF, near infrared fluorescence imaging. ***Agent*** – HAC, high affinity consensus; GNPs, gold nanoparticles; Mb, minibody; Nbs, nanobodies; cDb, Cys-diabody; mAB, monoclonal antibody; ScFV, single chain variable fragment; SPION, super paramagnetic iron oxide nanoparticle; CLIO, cross-linked iron oxide; GFP, green fluorescent protein; FLuc, firefly luciferase; NP, nanoparticle; FAC, fluoroarabinofuranosyl-cytosine; AraG, fluoroarabinofuranosyl-cytosine; dCK, deoxy-cytidine kinase; dGK, deoxy-guanosine kinase; TK1, thymidine kinase 1; FLT, fluorothymidine; FHBG, Fluoro-3-hydroxymethylbutyl guanine; NIS, sodium iodide symporter.